A Letters Journal Exploring the Frontiers of Physics

OFFPRINT

Excitonic resonances in the 2D extended Falicov-Kimball model

V.-N. Phan, H. Fehske and K. W. Becker

EPL, **95** (2011) 17006

A Letters Journal Exploring the Frontiers of Physics

July 2011

EPL, **95** (2011) 17006
doi: 10.1209/0295-5075/95/17006

www.epljournal.org

Excitonic resonances in the 2D extended Falicov-Kimball model

V.-N. Phan[1], H. Fehske[1,2(a)] and K. W. Becker[3]

[1] *Institut für Physik, Ernst-Moritz-Arndt-Universität Greifswald - D-17489 Greifswald, Germany, EU*
[2] *School of Physics, University of New South Wales - Kensington 2052, Sydney NSW, Australia*
[3] *Institut für Theoretische Physik, Technische Universität Dresden - D-01062 Dresden, Germany, EU*

received 27 January 2011; accepted in final form 15 May 2011
published online 17 June 2011

PACS 71.10.Li – Excited states and pairing interactions in model systems
PACS 71.35.-y – Excitons and related phenomena
PACS 71.30.+h – Metal-insulator transitions and other electronic transitions

Abstract – Using the projector-based renormalization method we investigate the formation of the excitonic insulator phase in the two-dimensional (2D) spinless Falicov-Kimball model with dispersive f electrons and address the existence of excitonic bound states at high temperatures on the semiconductor side of the semimetal-semiconductor transition. To this end we calculate the imaginary part of the dynamical electron-hole pair susceptibility and analyze the wave vector and energy dependence of excitonic resonances emerging in the band gap. We thereby confirm the existence of the exciton insulator and its exciton environment within a generic two-band lattice model with local Coulomb attraction.

Introduction. – In solids, the Coulomb interaction binds conduction band electrons and valence band holes to excitons. Normally, excitonic quasiparticles do not form the ground state but electron-hole excitations that tend to decay on a very short time scale. At a semimetal-semiconductor transition, however, the conventional ground state of the crystal may become unstable with respect to a spontaneous formation of excitons, provided the overlap or band gap between the valence and conduction bands is small. Then, for low enough temperatures, these composite bosonic quasiparticles will condense into a macroscopic phase-coherent quantum state, thereby transforming the semimetallic or semiconducting configuration into an insulating one (cf. also fig. 1). This so-called excitonic insulator (EI) state was theoretically proposed more than four decades ago [1,2]; for recent reviews see [3,4]. The EI phase realized below the critical temperature T_{EI} can be perceived either as BCS condensate in the semimetal region or as Bose Einstein condensate in the semiconductor region [5].

The EI state is extremely rare in nature, so far there is no free of doubt realization in any material. At present, the most promising candidates are the quasi-2D transition-metal dichalgogenide $1T$-$TiSe_2$ and the pressure-sensitive mixed-valence rare-earth chalgogenide $TmSe_{0.45}Te_{0.55}$. In $1T$-$TiSe_2$, the excitonic condensate exerts a force on the lattice generating periodic ionic displacements [6]. For $TmSe_{0.45}Te_{0.55}$, Hall effect, thermal diffusivity and heat conductivity data give strong support for a Bose

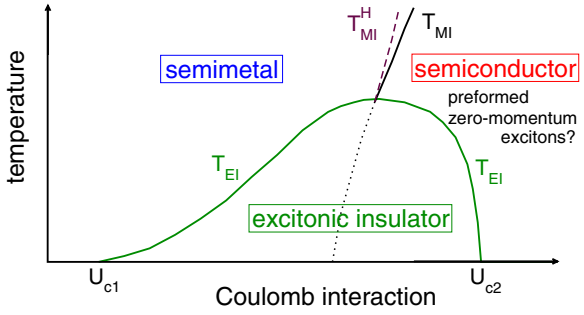

Fig. 1: (Color online) Schematic finite-temperature phase diagram of the EFKM as obtained from RPA [14] and slave-boson [15] approaches for the particle-hole asymmetric case $\varepsilon^f \neq \varepsilon^c$, $0 < |t^f| < t^c$. At the semimetal-semiconductor transition the ground state of the system may become unstable with respect to the spontaneous formation and condensation of excitons [2]. The strength of the Coulomb interaction determines on which side of the metal-insulator transition the system is. An interesting issue is the possible existence of preformed zero-momentum excitons in the semiconducting region for $T_{EI} < T < T_{MI}$, where T_{MI} denotes the critical temperature for the high-temperature metal-insulator transition. At T^H_{MI} the "Hartree" gap opens.

(a) E-mail: holger.fehske@physik.uni-greifswald.de

condensed state in the pressure range between 5 and 11 kbar below 20 K [7]. The transport anomalies observed at higher temperatures, in particular the strange increase of the electrical resistivity in a narrow pressure range around 8 kbar might be attributed to a free-bound state scattering in an exciton-rich "halo" of an EI [5]. As a basic prerequisite for the validity of this scenario, the existence of free excitons above the EI phase has to be proven, at least for the semiconducting region.

The aim of this paper is to address this issue. The investigation of Falicov-Kimball-type models seems to be minimal in this respect. The original Falicov-Kimball model describes localized f electrons and itinerant c electrons interacting by an on-site Coulomb interaction [8]. For our problem, we have to allow for a possible coherence between conduction band electrons and valence band holes however. This can be achieved either by including an explicit c-f hybridization [9] or a finite f bandwidth [10]. Indeed, using constrained path Monte Carlo [11] and mean-field [12] techniques, the 2D Falicov-Kimball model with direct f-f particle hopping has been shown to exhibit an excitonic ground state for intermediate Coulomb couplings provided that the center of the c and f bands, ε^c and ε^f, energetically differ. Note that around the symmetric case $\varepsilon^c = \varepsilon^f$ a charge-density-wave phase is energetically more stable [10–12]. Recent Hartree-Fock [13], RPA [14] and slave-boson [15] studies confirm this finding also for the 3D case. In this paper we use the projector-based renormalization method (PRM) [16,17] to calculate directly the excitonic pair susceptibility (up to second order in U). Analyzing the non-trivial frequency- and momentum dependence of $\chi(\mathbf{q},\omega)$ we are able to address the problem of exciton formation and condensation.

Theoretical approach. – In order to model the generic situation of semiconductors or semimetals with short-ranged attractive Coulomb interaction between conduction band (c) electrons and valence band (f) holes we consider an extended version of the Falicov-Kimball Hamiltonian (EFKM),

$$\mathcal{H} = \sum_{\mathbf{k}} \bar{\varepsilon}^c_{\mathbf{k}} c^\dagger_{\mathbf{k}} c_{\mathbf{k}} + \sum_{\mathbf{k}} \bar{\varepsilon}^f_{\mathbf{k}} f^\dagger_{\mathbf{k}} f_{\mathbf{k}} + U \sum_i n^c_i n^f_i \,, \qquad (1)$$

with two dispersive tight-binding bands $\bar{\varepsilon}^{c,f}_{\mathbf{k}} = \varepsilon^{c,f} - t^{c,f}\gamma_{\mathbf{k}} - \mu$. Here $\varepsilon^{c,f}$ are the on-site energies, $t^{c,f}$ are the nearest-neighbor particle transfer amplitudes, $\gamma_{\mathbf{k}} = 2\sum_d^D \cos k_d$ for a D-dimensional hypercubic lattice, and μ denotes the chemical potential. Accordingly the fermionic operators $c^{(\dagger)}_{\mathbf{k}}$ and $f^{(\dagger)}_{\mathbf{k}}$ annihilate (create) spinless c and f electrons with momentum $\mathbf{k}$, respectively, and n^c_i and n^f_i are the corresponding particle number operators for Wannier site i. U parametrizes the local Hubbard attraction. Note that if the c and f bands are degenerate, $\varepsilon^c = \varepsilon^f$ and $t^c = t^f$, the EFKM reduces to the standard Hubbard model [18], whereas for $t^f = 0$ the genuine FKM arises [8]. In the latter case the local f electron number is strictly conserved [13]. In what follows, we study the half-filled band case, with total electron density $\langle n\rangle = \langle n^c_i\rangle + \langle n^f_i\rangle = 1$. Moreover we consider a direct band gap situation with the maximum (minimum) of the c (f) band dispersion located at (π,π), *i.e.* $t^f < 0$. Without loss of generality the c electrons are considered to be "light" while the f electrons are "heavy", *i.e.* $|t^f| < 1$, where the c electron hopping integral is taken to be the unit of energy, $t^c = 1$, and $\varepsilon^c = 0$.

The projector-based renormalization approach starts from the decomposition of the many-particle Hamiltonian (1) into an 'unperturbed' part $\mathcal{H}_0$ (c and f electron band terms) and into a "perturbation" $\mathcal{H}_1$ (Coulomb interaction term), where the unperturbed part $\mathcal{H}_0$ clearly is solvable. Then, in general, $\mathcal{H}_1$ accounts for all transitions between the eigenstates of $\mathcal{H}_0$ with non-zero transition energies. Using a series of unitary transformations to integrate out the perturbation $\mathcal{H}_1$ (for details see ref. [16]) one arrives at a final Hamiltonian which is diagonal or at least quasi-diagonal. To evaluate the expectation value $\langle\mathcal{A}\rangle$ of any operator $\mathcal{A}$ also the operator has to be transformed by the same unitary transformation. One of the main advantages of the method is to find broken symmetry solutions of phase transitions [19]. Note that for practical applications the unitary transformations should best be done in small steps in energy. Therefore, the evaluation of the transformation in each small step can be restricted to low orders in $\mathcal{H}_1$. This procedure usually limits the validity of the renormalization approach to parameters values of $\mathcal{H}_1$ which are of the order of those of $\mathcal{H}_0$. In the present case, good agreement with exact results is expected for U values smaller than $t^{c,f}$ or $|\varepsilon^f_{\mathbf{k}} - \varepsilon^c_{\mathbf{k}}|$ (cf. eq. (4) below).

Excitonic insulator phase. – In a first step, let us address the formation of the long-range ordered EI state in the 2D EFKM. To this end we look for a non-vanishing excitonic expectation value $\langle c^\dagger f\rangle$, indicating a spontaneous symmetry breaking due the pairing of c electrons ($t^c > 0$) with f holes ($t^f < 0$). Employing the normal-ordered representation of fermionic operators $(:\ldots:)$, the Hamiltonian (1) reads $\mathcal{H} = \mathcal{H}_0 + \mathcal{H}_1$ with

$$\begin{aligned}\mathcal{H}_0 &= \sum_{\mathbf{k}} \varepsilon^c_{\mathbf{k}} :c^\dagger_{\mathbf{k}} c_{\mathbf{k}}: + \sum_{\mathbf{k}} \varepsilon^f_{\mathbf{k}} :f^\dagger_{\mathbf{k}} f_{\mathbf{k}}: \\ &\quad - \sum_{\mathbf{k}} (\Delta :f^\dagger_{\mathbf{k}} c_{\mathbf{k}}: + \text{H.c.}), \qquad (2)\\ \mathcal{H}_1 &= \frac{U}{N} \sum_{\mathbf{k}_1\mathbf{k}_2\mathbf{k}_3} :a_{\mathbf{k}_1\mathbf{k}_2\mathbf{k}_3}:,\end{aligned}$$

where

$$\Delta = \frac{U}{N} \sum_{\mathbf{k}} d_{\mathbf{k}}. \qquad (3)$$

Here $d_{\mathbf{k}} = \langle c^\dagger_{\mathbf{k}} f_{\mathbf{k}}\rangle$ plays the role of the EI order parameter, and $a_{\mathbf{k}_1\mathbf{k}_2\mathbf{k}_3} = c^\dagger_{\mathbf{k}_1} c_{\mathbf{k}_2} f^\dagger_{\mathbf{k}_3} f_{\mathbf{k}_1+\mathbf{k}_3-\mathbf{k}_2}$. Note that in $\mathcal{H}_0$, the on-site energies are shifted by a Hartree term,

$$\varepsilon^{c,f}_{\mathbf{k}} = \bar{\varepsilon}^{c,f}_{\mathbf{k}} + U\langle n^{f,c}\rangle, \qquad (4)$$

where $\langle n^c\rangle = \frac{1}{N}\sum_{\mathbf{k}}\langle c^\dagger_{\mathbf{k}} c_{\mathbf{k}}\rangle$ and $\langle n^f\rangle = \frac{1}{N}\sum_{\mathbf{k}}\langle f^\dagger_{\mathbf{k}} f_{\mathbf{k}}\rangle$ are the mean particle number densities of c and f electrons for a system with N lattice sites. Thus, $\mathcal{H}_0$ alone corresponds to the Hartree Hamiltonian. Vice versa, only fluctuation operators from the U term contribute to $\mathcal{H}_1$. Evaluating the expectation values $\langle\ldots\rangle$, the temperature enters into the calculation via the Fermi function, see [17].

Following the procedure of the PRM approach [17] by integrating out all transitions due to $\mathcal{H}_1$, the Hamiltonian $\mathcal{H}$ can be transformed to a fully renormalized Hamiltonian

$$\tilde{\mathcal{H}} = \sum_{\mathbf{k}} \tilde{\varepsilon}^c_{\mathbf{k}} : c^\dagger_{\mathbf{k}} c_{\mathbf{k}} : + \sum_{\mathbf{k}} \tilde{\varepsilon}^f_{\mathbf{k}} : f^\dagger_{\mathbf{k}} f_{\mathbf{k}} : + \sum_{\mathbf{k}} (\tilde{\Delta}_{\mathbf{k}} : f^\dagger_{\mathbf{k}} c_{\mathbf{k}} : + \text{H.c.}), \tag{5}$$

with modified parameters $\tilde{\varepsilon}^c_{\mathbf{k}}$, $\tilde{\varepsilon}^f_{\mathbf{k}}$, and $\tilde{\Delta}_{\mathbf{k}}$. Note that they take into account important correlation effects, which enter from the elimination procedure.

Self-evidently the single particle operators have to be transformed in order to evaluate expectation values, *i.e.*

$$: \tilde{c}^\dagger_{\mathbf{k}} : \; = \; \tilde{x}_{\mathbf{k}} : c^\dagger_{\mathbf{k}} : + \frac{U}{N} \sum_{\mathbf{k}_1\mathbf{k}_2} \tilde{y}_{\mathbf{k}_1\mathbf{k}\mathbf{k}_2} : c^\dagger_{\mathbf{k}_1} f^\dagger_{\mathbf{k}_2} f_{\mathbf{k}_1+\mathbf{k}_2-\mathbf{k}} :, \tag{6}$$

$$: \tilde{f}^\dagger_{\mathbf{k}} : \; = \; \tilde{x}'_{\mathbf{k}} : f^\dagger_{\mathbf{k}} : + \frac{U}{N} \sum_{\mathbf{k}_1\mathbf{k}_2} \tilde{y}'_{\mathbf{k}_1\mathbf{k}_2,\mathbf{k}-\mathbf{k}_1+\mathbf{k}_2}$$

$$\times : c^\dagger_{\mathbf{k}_1} c_{\mathbf{k}_2} f^\dagger_{\mathbf{k}-\mathbf{k}_1+\mathbf{k}_2} :, \tag{7}$$

where $\tilde{x}_{\mathbf{k}}$, $\tilde{y}_{\mathbf{k}}, \ldots$ are also renormalized parameters. In the PRM the renormalization results from integrating difference equations with initial conditions taken over from the original Hamiltonian 2 and the original single-particle operators: $\varepsilon^{c(f)}_{\mathbf{k},\Lambda} = \varepsilon^{c(f)}_{\mathbf{k}}$, $\Delta_{\mathbf{k},\Lambda} = 0^+$, $x_{\mathbf{k},\Lambda}(x'_{\mathbf{k},\Lambda}) = 1$, and $y_{\mathbf{k}_1\mathbf{k}_2\mathbf{k}_3,\Lambda}(y'_{\mathbf{k}_1\mathbf{k}_2\mathbf{k}_3,\Lambda}) = 0$.

The final Hamiltonian (5) can be diagonalized by a Bogoliubov transformation

$$\tilde{\mathcal{H}} = \sum_{\mathbf{k}} E^c_{\mathbf{k}} : c^\dagger_{\mathbf{k}} c_{\mathbf{k}} : + \sum_{\mathbf{k}} E^f_{\mathbf{k}} : f^\dagger_{\mathbf{k}} f_{\mathbf{k}} : + \tilde{E}\,, \tag{8}$$

where the quasiparticle energies are given by

$$E^{c/f}_{\mathbf{k}} = \frac{\tilde{\varepsilon}^c_{\mathbf{k}} + \tilde{\varepsilon}^f_{\mathbf{k}}}{2} \mp \frac{\text{sgn}(\tilde{\varepsilon}^f_{\mathbf{k}} - \tilde{\varepsilon}^c_{\mathbf{k}})}{2} W_{\mathbf{k}} \tag{9}$$

with $W_{\mathbf{k}} = [(\tilde{\varepsilon}^c_{\mathbf{k}} - \tilde{\varepsilon}^f_{\mathbf{k}})^2 + 4|\tilde{\Delta}_{\mathbf{k}}|^2]^{1/2}$.

A finite $\tilde{\Delta}_{\mathbf{k}}$ signals c-f electron coherence connected with a band gap that stabilizes the EI phase. Outside the EI phase, where $\tilde{\Delta}_{\mathbf{k}} = 0$, a band gap may also exist, provided that

$$E^{(0)}_g = E^c_{\mathbf{0}} - E^f_{\mathbf{0}} = \tilde{\varepsilon}^c_{\mathbf{0}} - \tilde{\varepsilon}^f_{\mathbf{0}}. \tag{10}$$

Therefore $E^{(0)}_g < 0$ ($E^{(0)}_g > 0$) may be taken as indication that the system is in the semimetallic (semiconducting) regime (cf. fig. 1). Let us emphasize that $E^{(0)}_g$ contains the fully renormalized quasiparticle energies $\tilde{\varepsilon}^{c,f}$, not just the Hartree energies $\varepsilon^{c,f}$ given by eq. (4).

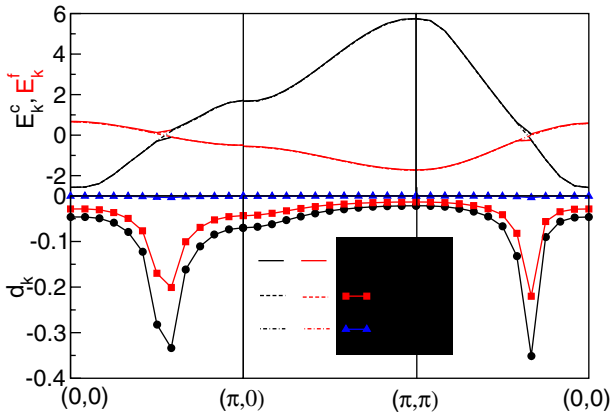

Fig. 2: (Color online) Quasiparticle dispersions $E^c_{\mathbf{k}}$ (black lines), $E^f_{\mathbf{k}}$ (red lines) (upper panel), and (b) "order-parameter" functions $d_{\mathbf{k}}$ (lower panel) along the major axes of the square lattice Brillouin zone. Results are calculated for $\varepsilon^f = -1.0$, $t^f = -0.3$, and $U = 2.0$ at various temperatures.

For the 2D tight-binding band case studied in this paper, we work on a discrete set of $N = 24 \times 24$ lattice sites and determine all quantities with a relative error of less than 10^{-5}.

Semimetallic region. Figure 2 (upper panel) shows the renormalized quasiparticle bands $E^c_{\mathbf{k}}$ and $E^f_{\mathbf{k}}$ along the high-symmetry axes of the 2D Brillouin zone, for $\varepsilon^f = -1$, $t^f = -0.3$, and $U = 2$. In this case, both bands overlap ($E^{(0)}_g < 0$) leading to a large Fermi surface, where both types of quasiparticles participate. At low temperatures a gap opens at the Fermi surface due to the formation of an excitonic insulating state. Such an EI state has been viewed before as a BCS condensate of loosely bound electron-hole pairs [5]. Increasing the temperature above some critical temperature T_{EI} the gap vanishes. At this temperature the EI-semimetal transition takes place. The lower panel of fig. 2 displays the order parameter function $d_{\mathbf{k}}$ as a function of $\mathbf{k}$. For low temperatures and $\mathbf{k}$ close to the Fermi surface, where both quasiparticle bands overlap, $d_{\mathbf{k}}$ is strongly peaked. Otherwise $d_{\mathbf{k}}$ is a rather smooth function of $\mathbf{k}$. As a matter of course, increasing T above T_{EI}, the order parameter function $d_{\mathbf{k}}$ vanishes.

In fig. 3 (panel (a)) the EI order parameter Δ (eq. (3)) is shown as a function of temperature for various values of ε^f at $U = 2$. Clearly seen is the formation of an EI state with non-zero Δ at low temperatures. The EI state is weakened by lowering ε^f since the overlap of c and f electron bands is reduced in this case. In panel (b), the temperature dependence of Δ is illustrated for various values of the Coulomb interaction U. Similar as before, the formation of an EI state is observed for low T. The EI region is decimated by lowering the c electron f hole attraction. One can assure oneself that the EI phase only appears in between some lower critical value U_{c1} and some upper critical value U_{c2} (on the semiconductor side, see below). In both panels of fig. 3, the solid blue lines give

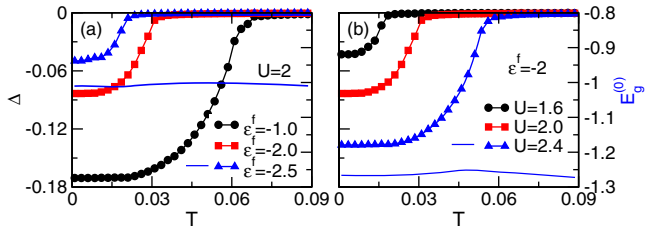

Fig. 3: (Color online) Temperature dependence of the EI order parameter Δ in (a) for various ε^f at $U=2$ and in (b) for various U at $\varepsilon^f=-2.0$, where $t^f=-0.3$. The solid lines give the variation of the gap $E_g^{(0)}$ (10) (note the scale on the right-hand side ordinate).

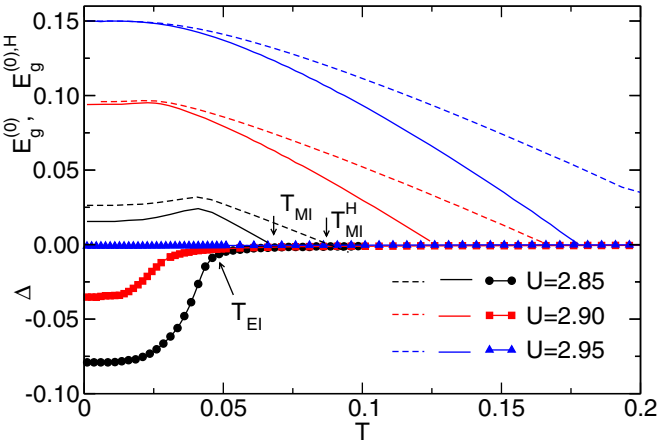

Fig. 4: (Color online) EI order parameter Δ (symbols) and energy gaps $E_g^{(0)}$ (solid lines), $E_g^{(0),H}$ (dashed lines) as functions of temperature for several values of the Coulomb interaction U where $\varepsilon^f=-2.4$, $t^f=-0.3$. T_{EI} and T_{MI} denote the critical temperatures for the EI transition and the metal-insulator transition, respectively. Note that directly opposed to fig. 3 the order parameter Δ decreases with increasing U in the semiconducting regime because the effective band overlap (necessary to establish c-f electron coherence) is now reduced on account of the Hartree term.

the variation of the negative quasiparticle gap $E_g^{(0)}$ with T, where $\varepsilon^f=-2.5$ in panel (a) and $U=2.4$ in (b). In either case, the variation of $E_g^{(0)}$ for small T towards lower values goes along with the formation of the EI state. For $U<U_{c1}$ the bare band splitting $\varepsilon^f-\varepsilon^c$ is somewhat reduced but $E_g^{(0)}$ is still negative, so we end up with a semimetallic situation.

Semiconducting region. We now discuss the possible appearance of an EI state on the semiconductor-side of the schematic phase diagram shown in fig. 1. Figure 4 displays the temperature dependence of the quasiparticle gap $E_g^{(0)}$ and the order parameter Δ for some larger values of U than before. The order parameter Δ is finite and negative at low T which again signals the existence of an EI phase. The EI phase in this region was interpreted as a BEC of preformed tightly bound excitons [5]. For T above the critical temperature T_{EI} the order parameter vanishes and no broken-symmetry state exists as in the semimetallic case. Note that $E_g^{(0)}$ is now positive at low temperatures, which indicates that we have a situation with a semiconductor-like band structure at least up to some critical temperature T_{MI}, where the band gap closes. Obviously, at T_{MI}, a semiconductor-semimetal metal-insulator transition occurs. We further note that due to the inclusion of correlation effects the PRM metal-insulator transition temperature T_{MI} strongly deviates from T_{MI}^H obtained by using the Hartree-shifted bare energies $\varepsilon_{\mathbf{k}}^{c,f}$ only, where $E_g^{(0),H}=E_{\mathbf{0}}^c-E_{\mathbf{0}}^f=\varepsilon_{\mathbf{0}}^c-\varepsilon_{\mathbf{0}}^f$ marks the corresponding Hartree band gap. The essential question whether exitonic bound states might possibly exist in the temperature region $T_{EI}<T<T_{MI}$ will be investigated below. In this connection, in ref. [5] the authors proposed a so-called "halo phase", where individual valence bond holes, conduction band electrons, and bound (but uncondensed) electron-hole pairs (excitons) should coexist.

Excitonic resonances. – To address the possible formation of excitonic bound states above T_{EI}, we analyze the frequency and momentum dependence of the dynamical excitonic susceptibility

$$\chi(\mathbf{q},\omega)=\langle\langle b_{\mathbf{q}};b_{\mathbf{q}}^\dagger\rangle\rangle(\omega), \tag{11}$$

where the symbol $\langle\langle\ldots\rangle\rangle$ denotes the retarded Green's function, and the creation operator of an electron-hole excitation with momentum $\mathbf{q}$ is defined by $b_{\mathbf{q}}^\dagger=\frac{1}{\sqrt{N}}\sum_{\mathbf{k}}c_{\mathbf{k}+\mathbf{q}}^\dagger f_{\mathbf{k}}$. Using the unitary invariance of expectation values, eq. (11) can be rewritten as

$$\chi(\mathbf{q},\omega)=\frac{1}{N}\sum_{\mathbf{k}\mathbf{k}'}\langle\langle\tilde{f}_{\mathbf{k}}^\dagger\tilde{c}_{\mathbf{k}+\mathbf{q}};\tilde{c}_{\mathbf{k}'+\mathbf{q}}^\dagger\tilde{f}_{\mathbf{k}'}\rangle\rangle_{\tilde{\mathcal{H}}}(\omega). \tag{12}$$

Here the two-particle Green's function on the right-hand side is formed with $\tilde{\mathcal{H}}$ and the quantities with tilde symbols are the fully renormalized operators. Taking into account that the EI order parameter vanishes for $T>T_{EI}$ ($\tilde{\Delta}_{\mathbf{k}}=0$, $\forall\,\mathbf{k}$), we obtain up to order $\mathcal{O}(U^2)$

$$\chi(\mathbf{q},\omega)=\frac{1}{N}\sum_{\mathbf{k}}\frac{\Gamma^0_{\mathbf{k}\mathbf{q}}}{\omega-\omega_{\mathbf{k}}(\mathbf{q})+i\eta}+\frac{1}{N^3}\sum_{\mathbf{k}\mathbf{k}_1\mathbf{k}_2}\left[\frac{\Gamma^1_{\mathbf{k}\mathbf{q}\mathbf{k}_1\mathbf{k}_2}}{\omega-E^{(1)}_{\mathbf{k}\mathbf{q}\mathbf{k}_1\mathbf{k}_2}+i\eta}-\frac{\Gamma^2_{\mathbf{k}\mathbf{q}\mathbf{k}_1\mathbf{k}_2}}{\omega-E^{(2)}_{\mathbf{k}\mathbf{q}\mathbf{k}_1\mathbf{k}_2}+i\eta}\right] \tag{13}$$

with

$$\omega_{\mathbf{k}}(\mathbf{q})=E^c_{\mathbf{k}+\mathbf{q}}-E^f_{\mathbf{k}}\,, \tag{14}$$

$$E^{(1)}_{\mathbf{k}\mathbf{q}\mathbf{k}_1\mathbf{k}_2}=E^c_{\mathbf{k}_1}-E^f_{\mathbf{k}}-E^f_{\mathbf{k}_1+\mathbf{k}_2-\mathbf{k}-\mathbf{q}}+E^f_{\mathbf{k}_2}\,, \tag{15}$$

$$E^{(2)}_{\mathbf{k}\mathbf{q}\mathbf{k}_1\mathbf{k}_2}=E^c_{\mathbf{k}+\mathbf{q}}-E^c_{\mathbf{k}_1}+E^c_{\mathbf{k}_2}-E^f_{\mathbf{k}-\mathbf{k}_1+\mathbf{k}_2}, \tag{16}$$

and $\eta = 0^+$. The coefficients Γ^i are given by

$$\begin{aligned}\Gamma^0_{\mathbf{kq}} &= \Big\{ |\tilde{x}'_{\mathbf{k}}\tilde{x}_{\mathbf{k+q}}|^2 \\ &- \frac{2U}{N}\sum_{\mathbf{k}_1} \tilde{x}'_{\mathbf{k}}\tilde{x}_{\mathbf{k+q}}(\tilde{x}_{\mathbf{k}_1+\mathbf{q}}\tilde{y}'_{\mathbf{k}_1+\mathbf{q},\mathbf{k}+\mathbf{q},\mathbf{k}}\langle\tilde{n}^c_{\mathbf{k}_1+\mathbf{q}}\rangle \\ &+ \tilde{x}'_{\mathbf{k}_1}\tilde{y}_{\mathbf{k}+\mathbf{q},\mathbf{k}_1+\mathbf{q},\mathbf{k}_1}\langle\tilde{n}^f_{\mathbf{k}_1}\rangle) \\ &+ \frac{U^2}{N^2}\sum_{\mathbf{k}_1\mathbf{k}_2}\Big[2\tilde{x}'_{\mathbf{k}}\tilde{x}_{\mathbf{k+q}}\tilde{y}_{\mathbf{k}_2,\mathbf{k}_1+\mathbf{q},\mathbf{k}_1-\mathbf{k}_2+\mathbf{k}+\mathbf{q}} \\ &\times \tilde{y}'_{\mathbf{k}_2,\mathbf{k}+\mathbf{q},\mathbf{k}_1-\mathbf{k}_2+\mathbf{k}+\mathbf{q}}\langle\tilde{n}^c_{\mathbf{k}_2}\rangle\langle\tilde{n}^f_{\mathbf{k}_1-\mathbf{k}_2+\mathbf{k}+\mathbf{q}}\rangle \\ &+ 2\tilde{x}'_{\mathbf{k}_1}\tilde{x}_{\mathbf{k}_2+\mathbf{q}}\tilde{y}_{\mathbf{k}_2,\mathbf{k}_1+\mathbf{q},\mathbf{k}_1}\tilde{y}'_{\mathbf{k}_2+\mathbf{q},\mathbf{k}+\mathbf{q},\mathbf{k}}\langle\tilde{n}^f_{\mathbf{k}_1}\rangle\langle\tilde{n}^c_{\mathbf{k}+\mathbf{q}}\rangle \\ &+ \tilde{x}_{\mathbf{k}_1+\mathbf{q}}\tilde{x}_{\mathbf{k}_2+\mathbf{q}}\tilde{y}'_{\mathbf{k}_2+\mathbf{q},\mathbf{k}+\mathbf{q},\mathbf{k}}\tilde{y}'_{\mathbf{k}_1+\mathbf{q},\mathbf{k}+\mathbf{q},\mathbf{k}} \\ &\times \langle\tilde{n}^c_{\mathbf{k}_1+\mathbf{q}}\rangle\langle\tilde{n}^c_{\mathbf{k}_2+\mathbf{q}}\rangle \\ &+ \tilde{x}'_{\mathbf{k}_1}\tilde{x}'_{\mathbf{k}_2}\tilde{y}_{\mathbf{k}+\mathbf{q},\mathbf{k}_2+\mathbf{q},\mathbf{k}_2}\tilde{y}_{\mathbf{k}+\mathbf{q},\mathbf{k}_1+\mathbf{q},\mathbf{k}_1}\langle\tilde{n}^f_{\mathbf{k}_1}\rangle\langle\tilde{n}^f_{\mathbf{k}_2}\rangle\Big]\Big\} \\ &\times (\langle\tilde{n}^f_{\mathbf{k}}\rangle - \langle\tilde{n}^c_{\mathbf{k}+\mathbf{q}}\rangle), \end{aligned} \tag{17}$$

$$\begin{aligned}\Gamma^1_{\mathbf{kqk}_1\mathbf{k}_2} &= U^2(|\tilde{x}'_{\mathbf{k}}\tilde{y}_{\mathbf{k}_1,\mathbf{k}+\mathbf{q},\mathbf{k}_2}|^2 \\ &- \tilde{x}'_{\mathbf{k}}\tilde{x}'_{\mathbf{k}_1+\mathbf{k}_2-\mathbf{k}-\mathbf{q}}\tilde{y}_{\mathbf{k}_1,\mathbf{k}+\mathbf{q},\mathbf{k}_2}\tilde{y}_{\mathbf{k}_1,\mathbf{k}_1+\mathbf{k}_2-\mathbf{k},\mathbf{k}_2}) \\ &\times \Big[\langle\tilde{n}^f_{\mathbf{k}}\rangle\langle\tilde{n}^f_{\mathbf{k}_1+\mathbf{k}_2-\mathbf{k}-\mathbf{q}}\rangle(1-\langle\tilde{n}^c_{\mathbf{k}_1}\rangle - \langle\tilde{n}^f_{\mathbf{k}_2}\rangle) \\ &- \langle\tilde{n}^f_{\mathbf{k}_2}\rangle\langle\tilde{n}^c_{\mathbf{k}_1}\rangle(1-\langle\tilde{n}^f_{\mathbf{k}}\rangle - \langle\tilde{n}^f_{\mathbf{k}_1+\mathbf{k}_2-\mathbf{k}-\mathbf{q}}\rangle)\Big], \end{aligned} \tag{18}$$

$$\begin{aligned}\Gamma^2_{\mathbf{kqk}_1\mathbf{k}_2} &= U^2(|\tilde{x}_{\mathbf{k}+\mathbf{q}}\tilde{y}'_{\mathbf{k}_1,\mathbf{k}_2,\mathbf{k}-\mathbf{k}_1+\mathbf{k}_2}|^2 \\ &- \tilde{x}_{\mathbf{k}+\mathbf{q}}\tilde{x}_{\mathbf{k}_2-\mathbf{q}}\tilde{y}'_{\mathbf{k}_1\mathbf{k}_2,\mathbf{k}-\mathbf{k}_1+\mathbf{k}_2}\tilde{y}'_{\mathbf{k}_1,\mathbf{k}+\mathbf{q},\mathbf{k}-\mathbf{k}_1+\mathbf{k}_2}) \\ &\times \Big[\langle\tilde{n}^c_{\mathbf{k}_2}\rangle\langle\tilde{n}^c_{\mathbf{k}+\mathbf{q}}\rangle(1-\langle\tilde{n}^f_{\mathbf{k}-\mathbf{k}_1+\mathbf{k}_2}\rangle - \langle\tilde{n}^c_{\mathbf{k}_1}\rangle) \\ &- \langle\tilde{n}^c_{\mathbf{k}_1}\rangle\langle\tilde{n}^f_{\mathbf{k}-\mathbf{k}_1+\mathbf{k}_2}\rangle(1-\langle\tilde{n}^c_{\mathbf{k}_2}\rangle - \langle\tilde{n}^c_{\mathbf{k}+\mathbf{q}}\rangle)\Big]. \end{aligned} \tag{19}$$

Here the expectation values $\langle\tilde{n}^c_{\mathbf{k}}\rangle = \langle c^\dagger_{\mathbf{k}}c_{\mathbf{k}}\rangle_{\tilde{\mathcal{H}}}$ and $\langle\tilde{n}^f_{\mathbf{k}}\rangle = \langle f^\dagger_{\mathbf{k}}f_{\mathbf{k}}\rangle_{\tilde{\mathcal{H}}}$, are formed with the renormalized Hamiltonian $\tilde{\mathcal{H}}$ and can easily be evaluated due to the diagonal form of $\tilde{\mathcal{H}}$. Note that the pole structure of the first (coherent) term of eq. (13) describes the continuum of particle-hole excitations. Of course, we have $\omega_{\mathbf{0}}(\mathbf{0}) = E^{(0)}_g$, and in view of the form of the c and f band dispersions $\omega_{\mathbf{k}}(\mathbf{0}) > \omega_{\mathbf{0}}(\mathbf{0})$, $\forall\,\mathbf{k} \neq \mathbf{0}$. Therefore the possibility of $\mathbf{q} = \mathbf{0}$ excitations with positive energy indicates that the system is in the semiconducting regime. If one tries to determine the semimetal-semiconductor boundary, *i.e.*, T_{MI}, from the pole structure of $\chi(\mathbf{q},\omega)$ this assertion is valid to leading order only; the second and third term of (13) might lead to a shift of the lowest excitation energy in the $\mathbf{q} = \mathbf{0}$ sector. As shown below, this effect is negligible however: the values of T_{MI} derived from $E^{(0)}_g$ are in accord with the results obtained from the dynamical susceptibility.

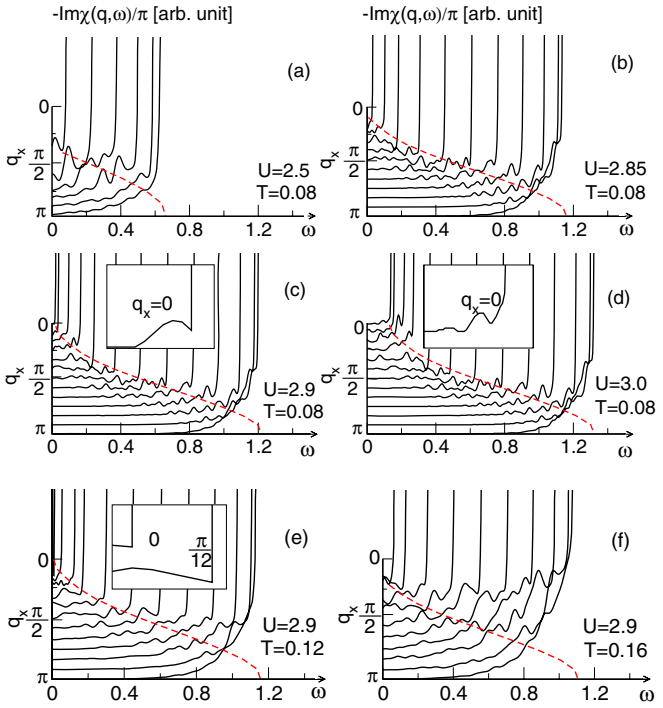

Fig. 5: (Color online) Imaginary part of the dynamical susceptibility $-\mathrm{Im}\,\chi(\mathbf{q},\omega)/\pi$ *vs.* frequency vertically shifted to show its values for different momenta along the $(q_x, 0)$-direction (black solid lines). The boundaries to the particle-hole continuum are marked by red dashed lines. The insets magnify the low-frequency small-momentum region whenever a gap appears for the electron-hole excitations. Bare band parameters are $\varepsilon^f = -2.4$, $t_f = -0.3$.

The imaginary part of $\chi(\mathbf{q},\omega)$ reads

$$\begin{aligned}-\frac{1}{\pi}\,\mathrm{Im}\,\chi(\mathbf{q},\omega) &= \frac{1}{N}\sum_{\mathbf{k}}\Gamma^0_{\mathbf{kq}}\delta[\omega - \omega_{\mathbf{k}}(\mathbf{q})] \\ &+ \frac{1}{N^3}\sum_{\mathbf{kk}_1\mathbf{k}_2}[\Gamma^1_{\mathbf{kqk}_1\mathbf{k}_2}\delta(\omega - E^{(1)}_{\mathbf{kqk}_1\mathbf{k}_2}) \\ &- \Gamma^2_{\mathbf{kqk}_1\mathbf{k}_2}\delta(\omega - E^{(2)}_{\mathbf{kqk}_1\mathbf{k}_2})], \end{aligned} \tag{20}$$

where possible non-zero excitations outside the particle-hole continuum point to the existence of excitonic resonances.

Figure 5 diplays our numerical results for the imaginary part of the exitonic susceptibility $-\mathrm{Im}\,\chi(\mathbf{q},\omega + i0)/\pi$ as a function of ω for different momenta $(q_x, 0)$ between $q_x = 0$ and π (black solid lines), indicated by the scale attached to the ordinate axis. In all panels the red dashed line represents the boundaries to the particle-hole continuum (indicated by the strong upturns). The small bumps in the figures correspond to excitonic resonances, where the maximum most closely located to the particle-hole continuum refers to an excitonic bound state.

In panels (a) to (d) the temperature is kept to $T = 0.08$. For $U = 2.5$, respectively, 2.85 (which are still larger than U_{c1} however), $T > T_{MI}$, and the system is in the

semimetallic region. No excitonic resonances can be found for $\mathbf{q}=0$ in this case, since $E_g^{(0)}$ is already negative (cf. fig. 4). There is a significant increase of the spectral weight of the finite-$\mathbf{q}$ excitonic resonances by going over from $U=2.5$ to $U=2.85$. In contrast, in panel (c), where $U=2.9$, we have $T_{EI}<T<T_{MI}$, and the system realizes a semiconductor (cf. figs. 1 and 4). Now a weak excitonic resonance is found at momentum $\mathbf{q}=0$ which can more clearly be seen from the inset. For $U=3.0>U_{c2}$ (panel (d)) the EI phase is not realized even for $T=0$ (cf. fig. 4), and again excitons can be formed for all values of q_x. Note that excitons with finite momentum $\mathbf{q}$ can be created in both semiconductor and semimetal cases (cf. panels (a) to (d)). Their resonance positions follow from eqs. (15) and (16).

In the two lowermost panels (e) and (f) the Coulomb interaction is fixed to $U=2.9$. Increasing the temperature from $T=0.12$ (e) to $T=0.16$ (f) the system passes the semiconductor-semimetal transition. Although, at $T=0.12$, the system is very close to the transition point (cf. fig. 4), excitons with zero momenta may form (see inset). In contrast, no $\mathbf{q}=0$ excitons can exist for the temperature considered in panel (f). Here we observe only excitonic resonances with finite momenta. For the higher-temperature case these resonances are more smeared out and their weight is enhanced. Therefore excitonic states with $\mathbf{q}\neq 0$ can easier be occupied for this case.

Figure 5 clearly shows that it is possible to extract the temperature T_{MI} just as well by monitoring the appearance of excitonic resonances in the imaginary part of $\chi(\mathbf{q},\,\omega+i0)$ at $\mathbf{q}=0$.

Conclusions. – In summary, we have performed a detailed investigation of the two-dimensional extended Falicov-Kimball model by means of the projector-based renormalization method. Thereby we established the long-predicted existence of an intervening excitonic insulator phase at the semimetal-semiconductor transition below some critical T_{EI} (see fig. 1). We derived the renormalized quasiparticle band structure which shows a correlation-induced single-particle gap and c-f electron coherence in the low-temperature EI state and reflects the metal-insulator transition at T_{MI} for higher temperatures. Analyzing the imaginary part of the excitonic pair susceptibility, we demonstrate that on the semiconductor side of this phase transition, preformed excitons with zero momentum exist above T_{EI}. On the other hand, excitonic bound states (resonances) with finite momentum may appear on both —semiconducting and semimetallic— sides of the metal-insulator transition, but these excitons will not condense for the studied direct band gap situation. We therefore corroborate the scenario, suggested by Bronold and Fehske [5], that in the semiconducting region the EI phase is surrounded by an excitonic halo consisting of free electrons, holes and tightly bound zero-momentum excitons. Forming the EI state, the latter undergo a Bose-Einstein condensation state as the temperature is lowered. Contrariwise there is a well-defined (large) Fermi surface in the semimetallic regime, and the EI state can be envisaged as composed of BCS-type electron-hole pairs.

* * *

The authors would like to thank F. X. Bronold, D. Ihle, H. Stolz, and B. Zenker for valuable discussions. HF acknowledges a Gordon Godfrey fellowship by the UNSW, where this work was completed. Research was supported by the DFG through SFB 652.

REFERENCES

[1] Mott N. F., *Philos. Mag.*, **6** (1961) 287; Knox R., in *Solid State Physics*, edited by Seitz F. and Turnbull D. (Academic Press, New York) 1963, Suppl. 5, p. 100; Keldysh L. V. and Kopaev H. Y. V., *Sov. Phys. Solid State*, **6** (1965) 2219; Jérome D., Rice T. M. and Kohn W., *Phys. Rev.*, **158** (1967) 462.

[2] Kohn W., in *Metals and Insulators* in *Many Body Physics*, edited by de Witt C. and Balian R. (Gordon & Breach, New York) 1968.

[3] Littlewood P. B. *et al.*, *J. Phys.: Condens. Matter*, **16** (2004) S3597.

[4] Monney C. *et al.*, *New J. Phys.*, **12** (2010) 125019.

[5] Bronold F. X. and Fehske H., *Phys. Rev. B*, **74** (2006) 165107.

[6] Monney C. *et al.*, *Phys. Rev. Lett.*, **106** (2011) 106404.

[7] Neuenschwander J. and Wachter P., *Phys. Rev. B*, **41** (1990) 12693; Bucher B., Steiner P. and Wachter P., *Phys. Rev. Lett.*, **67** (1991) 2717; Wachter P., Bucher B. and Malar J., *Phys. Rev. B*, **69** (2004) 094502.

[8] Falicov L. M. and Kimball J. C., *Phys. Rev. Lett.*, **22** (1969) 997; Ramirez R., Falicov L. M. and Kimball J. C., *Phys. Rev. B*, **2** (1970) 3383.

[9] Kanda K., Machida K. and Matsubara T., *Solid State Commun.*, **19** (1976) 651; Portengen T., Östreich T. and Sham L. J., *Phys. Rev. Lett.*, **76** (1996) 3384.

[10] Batista C. D., *Phys. Rev. Lett.*, **89** (2002) 166403.

[11] Batista C. D., Gubernatis J. E., Bonča J. and Lin H. Q., *Phys. Rev. Lett.*, **92** (2004) 187601.

[12] Farkašovský P., *Phys. Rev. B*, **77** (2008) 155130.

[13] Schneider C. and Czycholl G., *Eur. Phys. J. B*, **64** (2008) 43.

[14] Ihle D. *et al.*, *Phys. Rev. B*, **78** (2008) 193103.

[15] Brydon P. M. R., *Phys. Rev. B*, **77** (2008) 045109; Zenker B., Ihle D., Bronold F. X. and Fehske H., *Phys. Rev. B*, **81** (2010) 115122; **83** (2011) 235123.

[16] Becker K. W., Hübsch A. and Sommer T., *Phys. Rev. B*, **66** (2002) 235115; Sykora S., Becker K. W. and Fehske H., *Phys. Rev. B*, **81** (2010) 195127.

[17] Phan V.-N., Becker K. W. and Fehske H., *Phys. Rev. B*, **81** (2010) 205117.

[18] Hubbard J., *Proc. R. Soc. London, Ser. A*, **276** (1963) 238.

[19] Sykora S. and Becker K. W., *Phys. Rev. B*, **80** (2009) 014511; Sykora S., Hübsch A. and Becker K. W., *EPL*, **85** (2009) 57003.